Wind and Structures, Vol. 1, No. 4 (1998) 337-349
DOI: http://dx.doi.org/10.12989/was.1998.1.4.337

Numerical and experimental simulation of the wind field in the EXPO '98 area

A.D. Ferreira†

Mechanical Engineering Department, University of Coimbra, Polo II, 3030 COIMBRA, Portugal

A.C.M. Sousa‡

Mechanical Engineering Department, University of New Brunswick, P.O. Box 4400, Fredericton, NB, E3B 5A3, Canada

D.X. Viegas‡

Mechanical Engineering Department, University of Coimbra, Polo II, 3030 COIMBRA, Portugal

Abstract. A numerical and experimental study was performed for the wind flow field in one area, comprising a group of several pavilions separated by passageways, of the EXPO '98 - a World Exposition (Lisbon, Portugal). The focus of this study is the characterization of the flow field to assess pedestrian comfort. The predictions were obtained employing the Reynolds averaged Navier-Stokes equations with the turbulence effects dealt with the *k-ε RNG* model. The discretization of the differential equations was accomplished with the control volume formulation in a Cartesian coordinate system, and an advanced segregated procedure was used to achieve the link between continuity and momentum equations. The evaluation of the overall numerical model was performed by comparing its predictions against experimental data for a square cylinder placed in a channel. The predicted values, for the practical geometry studied, are in a good agreement with the experimental data, showing the performance and the reliability of the *k-ε RNG* model and suggesting that the numerical simulation is a reliable methodology to provide the required information.

Key words: pedestrian comfort; wind around buildings; interference; numerical simulation; *k-ε RNG* model.

1. Introduction

The impact of wind conditions upon pedestrian comfort has been a major concern of urban designers and planners, and the topic of considerable ongoing research (Durgin 1997, Soligo *et al.* 1997). The construction of a new structure (e.g., building, tower, or overpass) in an urban area may alter the overall wind patterns, however it is still a formidable task to have detailed, reliable information about local wind characteristics, which can strongly affect pedestrian comfort, and air

† Assistant Professor
‡ Professor

pollution accumulation and dispersion.

A further challenge in this field of work is related to the design of large areas of leisure and recreation. In general, they are characterised by long "residence times" and by a somewhat

Fig. 1 South-North aerial view of the EXPO '98 area, showing the South International Area in the centre of the picture (photo provided by Parque EXPO '98 SA)

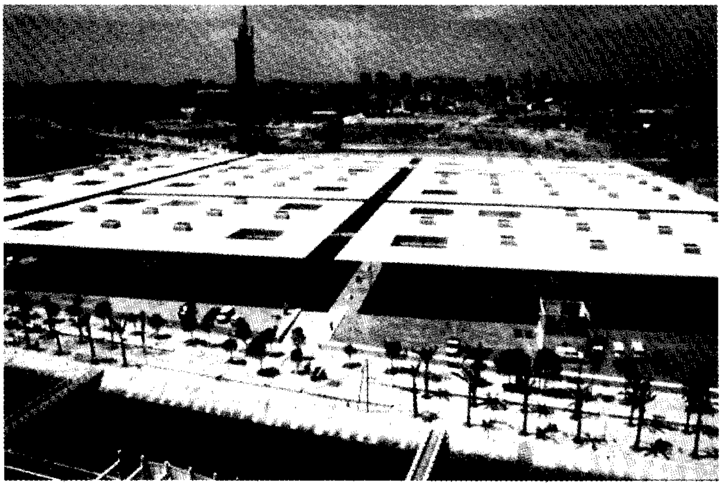

Fig. 2 East-west view of the South International Area (photo provided by Parque EXPO '98)

subjective concept of "high level of comfort". In any case, the particular environmental factors are of foremost importance, and critical at all stages of the design decision process stream, which needs to be supported by detailed information data. Data, which can be obtained through physical modelling in wind tunnel, however, and despite the expected quality of the results, the method is not free of pitfalls. Above all, wind tunnel runs are time consuming and costly and, depending on the complexity of the construction, detailed measurements may be impossible of carrying out for locations which are inaccessible to the instrumentation. Also, it should be mentioned that other costs and difficulties could arise from the construction of the models and appropriate wind tunnels are not widely available. A viable alternative is to obtain the data for the flow around the intervening structures via computational fluid dynamics (CFD), a procedure that requires the solution of the partial-differential equations governing momentum and continuity. Nevertheless, the technique should be used with caution due to the still-remaining CFD limitations in what concerns geometry complexity, and applicability and accuracy of turbulence models.

This paper presents some of the results from the study of the wind flow characterization around several pavilions (South International Area), placed in the south-side end of EXPO '98, a World Exposition held in Lisbon, from May to September 1998. The study was carried out at the request of the Energy Office (Núcleo de Energia) of the Parque EXPO '98 SA, and it encompasses the two approaches already outlined : physical (wind tunnel) and numerical (CFD) modelling. Fig. 1 shows an aerial view of the EXPO '98 area; in the centre of the picture, South International Area, which is displayed in a closer view in Fig. 2.

2. Description of the configuration studied

The site of the EXPO '98 is located on the north bank of the Tagus River, with a total approximate area of 2×1.5 km^2, in nearly flat land. Wind records over several years indicate that the prevailing winds are in the north-south direction.

A global wind characterization study was performed for the full EXPO '98 site using a 1:500-

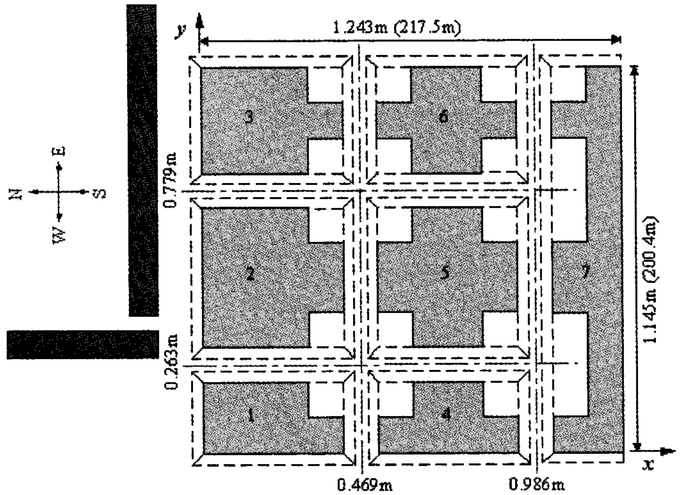

Fig. 3 Schematic representation of a top view of the construction in the area being studied. The dimensions within brackets correspond to those of the actual site; the others are those of the 1:175 model

Fig. 4 Schematic representation of a East side view, $h1$=0.052 m (9.1 m); $h2$=0.008 m (1.4 m) (the vertical scale is twice the horizontal scale)

scale model (Viegas *et al.* 1997). However, the present study is addressed to a particular area of the site where the seven pavilions, separated by passageways, are located. Figs. 3 and 4 show two schematic views of the area studied, with an indication of actual and model dimensions, and the location of the midplane of each passageway. Fig. 3 also indicates, with dashed lines, the overhangs of the pavilion's roofs which partly cover the passageways. Buildings R1 and R2 represent two auxiliary areas (information centres and restaurants), and because of their proximity to the pavilions, they were also taken in account in the study. Due to the large difference between the horizontal and vertical dimensions, the right view, shown in Fig. 4, was drawn with a vertical scale twice as large as the horizontal scale.

3. Methodologies

3.1. Physical modelling

The model, Figs. 3 and 4, was constructed to the scale 1:175, with global dimensions of 2× 2.1 m^2. A single hot film probe was used to determine vertical velocity profiles at different locations inside of the passageways y=0.263 m and y=0.779 m. As the probe required alignment with the wind direction, only the north-wind direction was tested. In order to obtain additional information concerning the magnitude and direction of the velocity, several vertical and horizontal profiles, for north and northeast directions, were done using a seven-hole probe (Silva and Viegas 1994). Due to the seven-hole probe's size, and in order to reduce the interference effect with the ground, the horizontal profiles were measured at z=0.017 m, corresponding to a full-scale height of 3 m. For the "free stream" velocity, a wind power profile

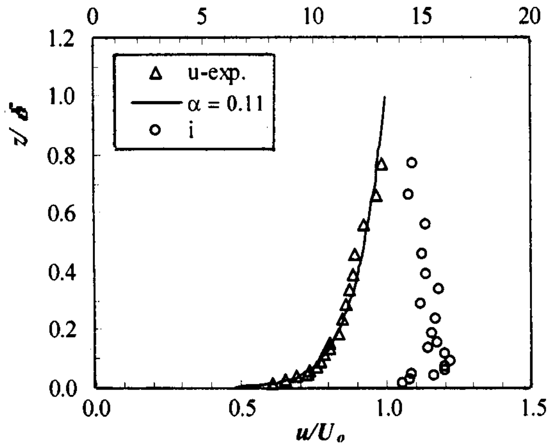

Fig. 5 Velocity and turbulence intensity profiles measured in the wind tunnel

was assumed to be valid, namely :

$$\frac{u}{U_o} = \left(\frac{z}{\delta} \right)^{\alpha} \tag{1}$$

for which the exponent α was found to be around 0.11, corresponding to the flow over nearly flat terrain or a large body of water conditions.

Fig. 5 shows the nondimensional wind profile ($U_o = 11$ m/s, $\delta = 0.40$ m), and turbulence intensity (i) defined by $i = \sqrt{\overline{u'^2}} / U_o$, measured 0.5 m away from the model's pavilions 1 and 3 in the wind tunnel. The symbols U_o and δ represent the outside boundary layer velocity and the thickness of that layer, respectively. In order to generate the profile shown, and due to the short length of the working section (5.5 m length, 2 m width) of the tunnel, only 0.3 m-height vorticity generators (Counihan 1973) were used.

3.2. Numerical simulation

The wind flow through the passageways was assumed to be governed by the three-dimensional, incompressible, turbulent, steady-state equations of conservation of mass and momentum. These equations, continuity and Navier-Stokes equations, can be formulated as follows :

$$\frac{\partial u_i}{\partial x_i} = 0 \tag{2}$$

$$\frac{\partial}{\partial x_j}(\rho u_j u_i) = -\frac{\partial p}{\partial x_i} + \frac{\partial}{\partial x_j}\left[\mu \left(\frac{\partial u_i}{\partial x_j} + \frac{\partial u_j}{\partial x_i} \right) - \rho \overline{u_i' u_j'} \right] \tag{3}$$

The standard formulation of the k-ε model (Launder and Spalding 1974) was adopted as the base form for the evaluation of the Reynolds stress tensor $-\rho \overline{u_i' u_j'}$. Using the eddy viscosity concept, where $\mu_t = C_\mu \rho k^2 / \varepsilon$, the model is expressed by the following equations :

$$-\rho \overline{u_i' u_j'} = \mu_t \left(\frac{\partial u_i}{\partial x_j} + \frac{\partial u_j}{\partial x_i} \right) - \frac{2}{3} \delta_{ij} \left(\mu_t \frac{\partial u_k}{\partial x_k} + \rho k \right) \tag{4}$$

$$\frac{\partial}{\partial x_j}(\rho u_j k) = \frac{\partial}{\partial x_j}\left[\left(\mu + \frac{\mu_t}{\sigma_k} \right) \frac{\partial k}{\partial x_j} \right] + \mu_t \left(\frac{\partial u_i}{\partial x_j} + \frac{\partial u_j}{\partial x_i} \right) \frac{\partial u_i}{\partial x_j} - \rho \varepsilon \tag{5}$$

$$\frac{\partial}{\partial x_j}(\rho u_j \varepsilon) = \frac{\partial}{\partial x_j}\left[\left(\mu + \frac{\mu_t}{\sigma_\varepsilon} \right) \frac{\partial \varepsilon}{\partial x_j} \right] + C_{\varepsilon 1} \frac{\varepsilon}{k} \mu_t \left(\frac{\partial u_i}{\partial x_j} + \frac{\partial u_j}{\partial x_i} \right) \frac{\partial u_i}{\partial x_j} - C_{\varepsilon 2} \rho \frac{\varepsilon^2}{k} \tag{6}$$

The *RNG* (renormalization group) extension of the k-ε model, proposed by Yakhot *et al.* (1992), was chosen for the turbulence modelling, according to several test cases performed by the authors for flow around bluff bodies, namely a cube immersed in a boundary layer and fully-

Table 1 Turbulence model constants value

Model	C_μ	$C_{\varepsilon 1}$	$C_{\varepsilon 2}$	σ_k	σ_ε	η_o	β
k-ε standard	0.09	1.45	1.9	1.0	1.3	--	--
k-ε *RNG*	0.085	1.42	1.68	0.72	0.72	4.38	0.015

developed flow over cylinders of square cross-section as shown in the Section "Turbulence Model Testing". The *RNG* model provides an improvement, as compared to the k-ε model, in flows where recirculation zones occur, a finding of the present study, and corroborated by other authors (e.g., Rokni 1998, Pakehal *et al.* 1994). The *RNG* model differs from the k-ε standard model by the inclusion of an extra term in the right hand side of the dissipation transport Eq. (6). The extra term R depends on the rate of strain, and is formulated as :

$$R = -\frac{\rho C_\mu \eta^3 (1-\eta/\eta_o)}{1+\beta\eta^3}\frac{\varepsilon^2}{k} \tag{7}$$

where $\eta = Sk/\varepsilon$, $S^2 = 2S_{ij}S_{ij}$, being S_{ij} the mean strain tensor. The different constants are set according to Table 1.

The control volume formulation (Patankar 1980) was chosen for the discretization of the transport equations in a Cartesian coordinate system. Continuity and momentum equations are linked through pressure in accordance with the SIMPLEC formulation (Van Doormall and Raythby 1984). The code is based on the CANYON (Lopes *et al.* 1995) software, however appropriate changes were made to accommodate the implementation of new routines and procedures.

The experimental values measured in the wind tunnel for the streamwise velocity (u) were used for the inlet boundary conditions for velocity and turbulent kinetic energy (k). For the dissipation and turbulent viscosity, at the entrance, the procedure proposed in Murakami *et al.* (1996) was adopted. The boundary conditions near the solid walls were implemented using wall functions as proposed in Versteeg and Malalasekera (1995), while all variables were assumed to have a zero-gradient normal to the computational outflow area.

For the calculations, a Pentium 233 MHz, with 96 MB of RAM memory was used. In order to simulate the entire computational domain, a total of ($95 \times 95 \times 34$) grid points were taken over a non-uniform mesh with mesh refinement in the vicinity of all the solid surfaces. A low-Reynolds number model (Nagano and Hishida 1987), if it had been used, would require a further refinement of the grid. Numerical tests conducted by the authors for a cylinder clearly demonstrate that the performance of this model deteriorates rapidly if at least a few grid nodal points are not inside the viscous sublayer.

For the simulations presented in the present study, typical times required to satisfy the convergence criteria, i.e., the residual of mass is less than 1% of the inflow mass, and the total Euclidean residue is less than 1% of the initial residue for all other variables, were around 10 hours.

4. Turbulence model testing

In order to evaluate the performance of the turbulence model chosen, the benchmark described

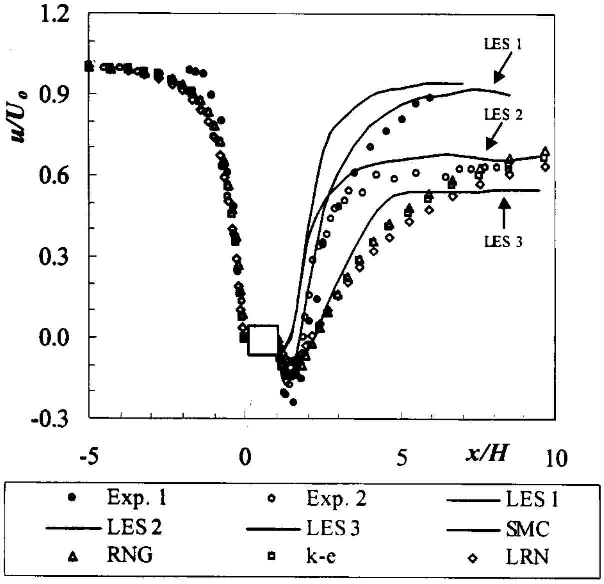

Fig. 6 Nondimensional velocity distribution along the axial longitudinal symmetry line of a 2D square cross section cylinder. Exp. 1 (Durão *et al.* 1988); Exp. 2 (Lyn *et al.* 1995); LES distributions; 1-Archambeau *et al.*, 2-Tamura *et al.*, 3-Kawamura and Kawashima (Table 3 and Fig. 4 of Rodi *et al.* 1997); SMC (Franke and Rodi 1993)

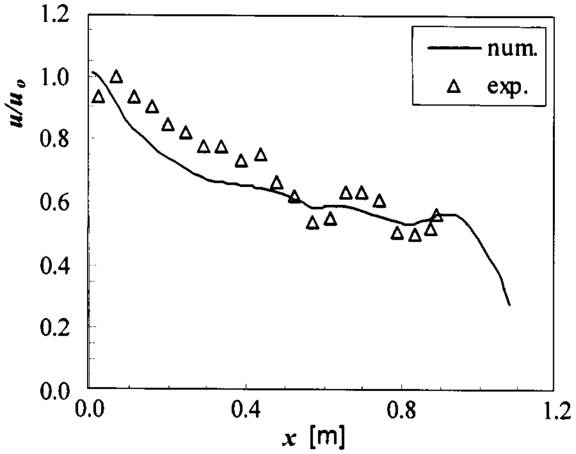

Fig. 7 Velocity magnitude distribution at y=0.263 m and z=0.017 m, for N-wind direction

in Freitas (1995) was performed, among other tests for flow around a bluff body. The results are shown in Fig. 6, where experimental results (Durão *et al.* 1988, and Lyn *et al.* 1995) are compared with those obtained by using the Large Eddy Simulation (LES) (Rodi *et al.* 1997), Second Moment Closure (SMC) (Franke and Rodi 1993), together with the authors' results employing the *k-ε RNG* (RNG), standard *k-ε* (k-e) and low-Reynolds number (LRN) models. Results obtained by three different research groups (Archambeau, Laurence and Leschziner-France and U.K.; Tamura, Itoh and Takakuwa-Japan; Kawamura and Kawashima-Japan) using the *LES*

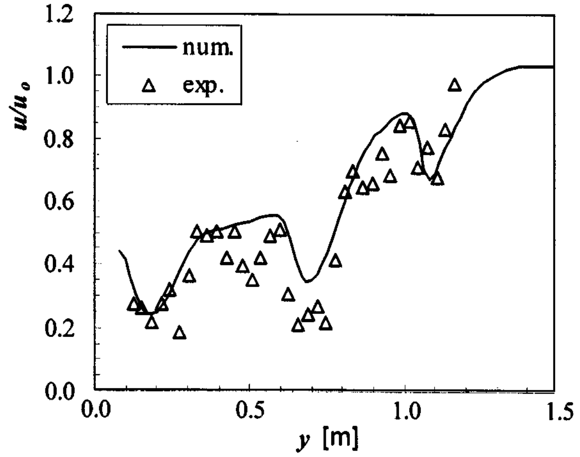

Fig. 8 Velocity magnitude distribution at x=0.469 m and z=0.017 m, for the NE-wind direction

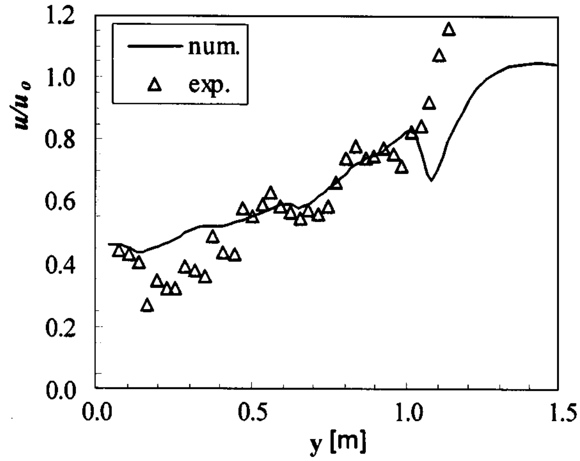

Fig. 9 Velocity magnitude distribution at x=0.986 m and z=0.017 m, for the NE-wind direction

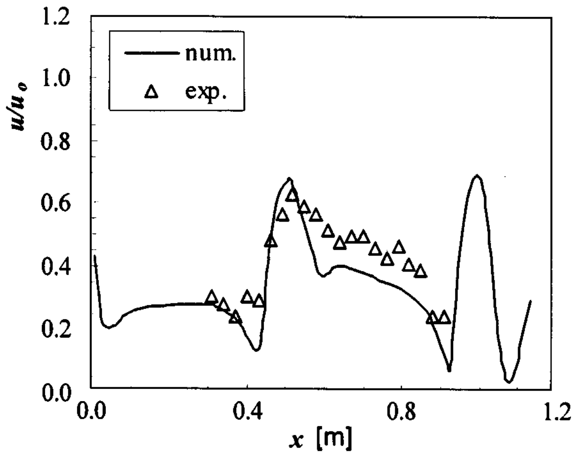

Fig. 10 Velocity magnitude distribution at y=0.779 m and z=0.017 m, for the NE-wind direction

approach, as reported by Rodi *et al.* 1997, are also included in Fig. 6. The *RNG* model, beyond the computational advantage of a two-equation turbulence model, provides acceptable results when compared to those obtained with *LES* or *SMC* models.

5. Results and discussion

The performance of the numerical model was evaluated by comparing the predictions against the experimental results for the horizontal profiles measured with the seven-hole probe, for two different incidence directions : north (N) and northeast (NE). The results are shown in Figs. 7 to 10, for different passageways. All the values are related to the model's height of 0.017 m measured from the ground (the actual site dimension is 3 m). In the figures, it is only represented the ratio between the magnitude of the velocity (*u*), divided by that of the non-disturbed velocity

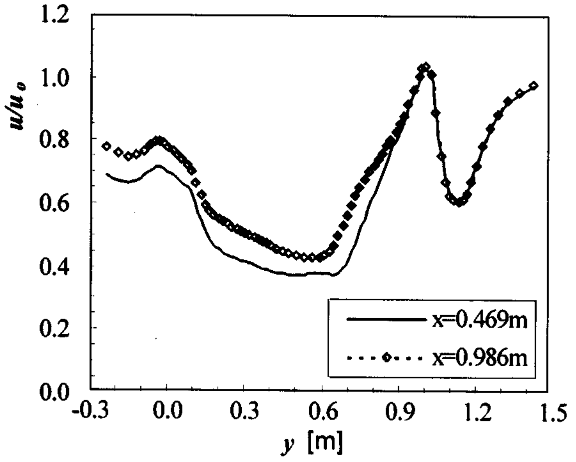

Fig. 11 Velocity magnitude distribution in two passageways, at z=0.017 m, for the E-wind direction

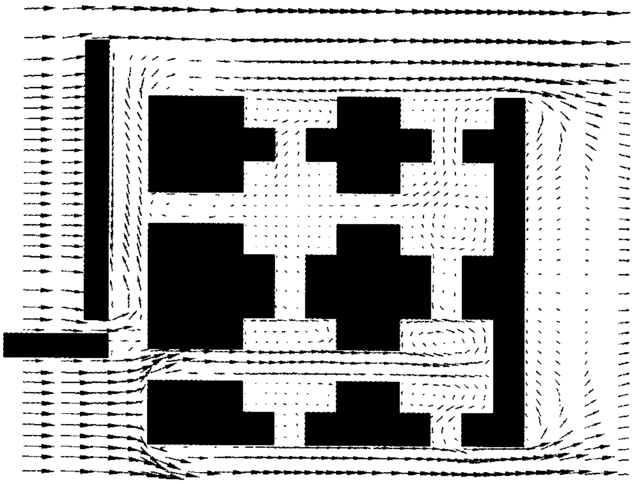

Fig. 12 Vectorial representation of the wind field at z=0.017 m, for the N-wind direction

at the same height (u_o), obtained from Eq. (1), for $z = 0.017$ m. The flow is inherently three-dimensional flow, however the particular geometry of the pavilions' roofs has a pronounced influence upon the vertical velocity component as compared to the horizontal, particularly close to the ground. Therefore, some of the figures just show the top view of the velocity field. The visualisation of the vector plots was accomplished with the software package Flowvis (Lopes 1997).

The experimental and numerical trends are generally in a good agreement, however it can be noticed a few minor discrepancies, some of them can be attributed to uncertainties associated with the experimental results as well as limitations of the numerical model. For instance, in Fig. 9, for y larger than 1.0 m, the discrepancy between experiments and predictions may be due to the limitations of the probe in what concerns the high angle between its alignment and wind flow

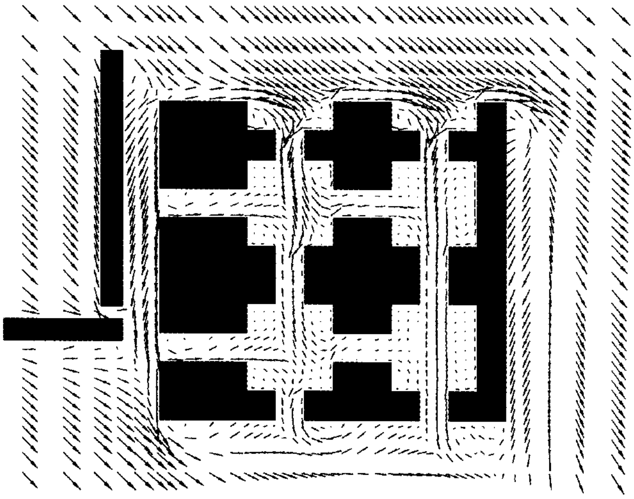

Fig. 13 Vectorial representation of the wind field at z=0.017 m, for the NE-wind direction

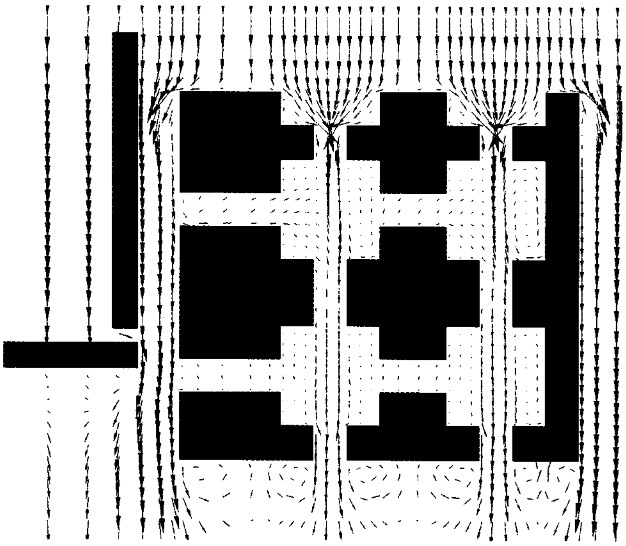

Fig. 14 Vectorial representation of the wind field at z=0.017 m, for the E-wind direction

direction, and to the location itself in the wind tunnel - preliminary tests performed in the wind tunnel working section indicated a non uniform distribution of velocity, particularly around the edges. Also, the occurrence of a peak for x larger than approximately 0.9 m, shown in Fig. 10, was not possible to verify experimentally because that area was not accessible to the seven-hole probe. Fig. 11 indicates that, for the eastern-wind direction, the velocity profiles are similar in the passageways x=0.469 m and x=0.986 m, respectively, in particular at the entrance region where the flow is practically undisturbed by the entraining "side-flows".

For the north wind direction, the worst conditions in terms of comfort are expected to occur in the vicinity of the entrance of the passageway between pavilions 1 and 2, as a result of the alignment of this passageway, and of the flow channelling into the narrow space by the structure R2. This is corroborated by Fig. 12, which depicts the predicted wind field for $z = 0.017$ m. According to experimental and numerical results, not shown here, the structure R1 behaves as a shelter barrier, protecting passageway $y = 0.779$ m from eventual strong wind velocities.

When the wind is blowing in the northeast-southwest direction, as shown in Figs. 8, 9, 10 and 13, the highest velocities do occur, as expected, on the east side of the pavilions area, near the entrances of the passageways between pavilions 3 and 6, and 6 and 7. It is interesting to notice that along the passageway $y = 0.779$ m, two peaks occur, located around the alignments $x = 0.469$ m and 0.986 m. These relatively high values of the velocity are expected to be felt especially by those walking toward the north direction, due to the sudden change of velocity magnitude.

The configuration of the east-side pavilions 3, 6 and 7, and the absence of any protection from the river side, are expected to yield the worst conditions when the wind is blowing from east to west, as indicated by the numerical results shown in Figs. 11 and 14. The passageways behave as a kind of canyon, inducing strong winds, specially in the narrow pedestrian crossing passages, between buildings 3 and 6, and 6 and 7.

6. Conclusions

The paper describes the numerical and experimental methodology adopted for the study of the wind flow characterization inside a group of pavilions in the area of EXPO '98. Based on turbulence model tests performed, it was found that the *RNG* extension of the k-ε model provides an improvement specially in flows where recirculation zones are expected.

For the practical case of the EXPO '98, the comparison between measured and predicted results revealed a good agreement, corroborating the reliability of the *RNG* model. Different incidence angles were simulated, and it can be concluded that, for the eastern wind direction, wind velocity augmentation is expected to occur in some of the passageways, due to the absence of any protection barriers as well the geometry configuration of the pavilions located on the east-side of the area analysed. It can be concluded that the numerical approach was capable of providing the information requested by the EXPO '98 planners in an efficient and inexpensive manner.

Acknowledgements

The first author (ADF) acknowledges the fellowships received from Calouste Gulbenkian

Foundation and INVOTAN (NATO Research). The facilities provided by the University of New Brunswick and the support received by the project from Natural Sciences and Engineering Research Council of Canada, through the operating grant OGP0001396 (ACMS) are also acknowledged. The construction of the physical model was possible due to the expeditious effort and great skill of Mr. Alberto C.A. Santos. Finally, the tangible and intangible contributions made by Parque EXPO '98 SA to the project are gratefully acknowledged by the authors.

References

Counihan, J. (1973), "Simulation of an adiabatic urban boundary layer in a wind tunnel", *Atmospheric Environment*, **7**, 683-689.

Durão, D.G., Heitor, M.V., Pereira, J.C.F. (1988), "Measurements of turbulent and periodic flows around a square cross-section cylinder", *Exp. in Fluids*, **6**, 298-304.

Durgin, F.H. (1997), "Pedestrian level wind criteria using the equivalent average", *J. Wind Eng. Ind. Aerod.*, **66**, 215-226.

Franke, R., Rodi, W. (1993), "Calculations of vortex shedding past a square cylinder with various turbulence models", *Proceedings of the 8th Symposium on Turbulent Shear Flows*, Berlin, Germany.

Freitas, C.J. (1995), "Perspective : Selected benchmarks from commercial CFD codes", *J. Fluids Eng.*, **117**, 208-218.

Lakehal, D., Barré, C., Sacré, C. (1994), "Simulation of turbulent flows around 3-D structures with complex geometries", *International Symposium on Turbulence, Heat and Mass Transfer*, Lisbon, Portugal, 8.1.1-8.1.6.

Launder, B.E., Spalding, D.B. (1974), "The numerical computation of turbulent flows", *Comp. Meth. Applied Mech. Eng.*, **3**, 269-289.

Lopes, A.M.G. (1997), "FlowVis - CAD based solution for the graphical post-processing of scalar and vectorial data", *Environmental Modelling and Software*, **12**, 2-3, 161-168.

Lopes, A.M.G., Sousa, A.C.M., Viegas, D.X. (1995), "Numerical simulation of turbulent flow and fire propagation in complex topography", *Num. Heat Transfer*, Part A, **27**, 229-253.

Lyn, D.A., Einav, S., Rodi, W., Park, J.-H., 1995, "A laser-Doppler velocimetry study of ensemble-averaged characteristics of the turbulent near wake of a square cylinder", *J. Fluid Mechanics*, **304**, 285-319.

Murakami, S., Mochida, A., Ooka, R., Kato, S., Iizuka, S. (1996), "Numerical prediction of flow around a building with various turbulence models : comparison of *k-ε EVM, ASM, DSM*, and *LES* with wind tunnel tests", *ASHRAE Transactions*, **102**, 1, 741-753.

Nagano, Y., Hishida, M. (1987), "Improved form of the *k-ε* model for wall treatment shear flows", *J. Fluids Eng.*, **109**, 156-160.

Patankar, S.V. (1980). *Numerical Heat Transfer and Fluid Flow*, Hemisphere Publishing Corporation, Washington, D.C., 197.

Rodi, W., Ferziger, J.H., Breuer, M., Pourquié, M. (1997), "Status of large eddy simulation : results of a workshop", *J. Fluids Eng.*, **119**, 248-262.

Rokni, M. (1998), "Numerical investigation of turbulent fluid flow and heat transfer in complex ducts", PhD Thesis, Lund Institute of Technology, Lund, Sweden.

Silva, M. C. G.; Viegas, D. X. (1994), "Calibration and use of a non-nulling seven-hole pressure probe" - AGARD CP-535 - Wall Interference, Support Interference and Flow Field Measurements, 1-7.

Soligo, M.J., Irwin, A.P., Williams, C.J. (1997), "Comprehensive assessment of pedestrian comfort including thermal effects", *Proceedings of 8th National Conference on Wind Engineering*, John Hopkins University, Baltimore, Maryland, USA, 5-7 de June de 1997.

Van Doormaal, J.P., Raithby, G.D. (1984), "Enhancements of the SIMPLE method for predicting incompressible flow", *Num. Heat Transfer*, **7**, 147-163.

Versteeg, H.K., Malalasekera, W. (1995). *An Introduction to Computational Fluid Dynamics : The Finite*

Volume Method, Harlow, Essex, England : Longman Scientific & Technical; New York : Wiley, 257.
Viegas, D.X., Ferreira, A.D., Lopes, A.G., Mendes, J.F., Santos, O.S. (1997), "Experimental study of wind and pedestrian comfort in the area of EXPO '98", *Proceedings of 2nd EACWE*, Genova-Italy, 22-26 June 1997.
Yakhot, V., Orszag, S.A., Thangam, S., Gatski, T.B., Speziale, C.G. (1992), "Development of turbulence models for shear flows by a double expansion technique", *Physics of Fluids-A*, **4**, 1510-1520.

(Communicated by Chang-Koon Choi)